Experimental investigation of electromagnetic fields from Helmholtz type circular coils
by Michael William Sampsel

A thesis submitted in partial fulfillment of the requirements for the degree of MASTER OF SCIENCE in Electrical Engineering
Montana State University
© Copyright by Michael William Sampsel (1982)

Abstract:
The subject of this thesis is to measure spatial variations of electromagnetic fields from circular time varying current sources. In order to verify experimental measurements digital computer models of the fields in free space were derived. Fields within Ringer's solution contained within cylindrical and rectangular boundaries were measured experimentally. It was found that neither boundary provides for uniform field magnitudes throughout the containers regardless of the direction of the applied magnetic field from the circular current loops. A coaxial cylindrical container was suggested as a means of providing more uniform fields throughout the solution.

A brief Fourier analysis of several types of waveforms induced in the Ringer's solution was also performed.

STATEMENT OF PERMISSION TO COPY

In presenting this thesis in partial fulfillment of the requirements for an advanced degree at Montana State University, I agree that the Library shall make it freely available for inspection. I further agree that permission for extensive copying of this thesis for scholarly purposes may be granted by my major professor, or, in his absence, by the Director of Libraries. It is understood that any copying or publication of this thesis for financial gain shall not be allowed without my written permission.

Signature Michael W. Sampsel

Date May 10, 1982

EXPERIMENTAL INVESTIGATION OF ELECTROMAGNETIC FIELDS FROM HELMHOLTZ TYPE CIRCULAR COILS

by

MICHAEL WILLIAM SAMPSEL

A thesis submitted in partial fulfillment
of the requirements for the degree

of

MASTER OF SCIENCE

in

Electrical Engineering

Approved:

Bruce R. McLeod
Chairman, Examining Committee

D. A. Pierre
Head, Major Department

Michael Malone
Graduate Dean

MONTANA STATE UNIVERSITY
Bozeman, Montana

June, 1982

ACKNOWLEDGMENTS

The author extends appreciation and thanks to Dr. A. A. Pilla and Electro-Biology Inc. for the use of the BI-OSTEOGEM. The author would also like to thank Dr. Daniel March and Dr. Donald Pierre for their suggestions in the preparation of this paper. The author is especially grateful for Dr. Bruce R. McLeod's support, suggestions and encouragement throughout the project. Most of all the author is thankful for the support given from his wife and his parents.

TABLE OF CONTENTS

	Page
VITA	ii
ACKNOWLEDGMENTS	iii
TABLE OF CONTENTS	iv
LIST OF TABLES	vi
LIST OF FIGURES	vii
ABSTRACT	x
INTRODUCTION	1
Chapter	
I SPATIAL VARIATIONS OF ELECTRIC AND MAGNETIC FIELDS IN FREE SPACE	3
Theoretical Fields for Circular Current Loops	3
Selection Inductive Test Systems	5
Experimental Methods and Procedures	8
Theoretical and Experimental Results	12
Accuracy of Results	17
II FOURIER ANALYSIS	18
Current Density a Result of Fourier Analysis	21
III BOUNDARY CONDITION CONSIDERATIONS AN EXPERIMENTAL VIEW	30
Experimental Procedure	30
Experimental Results	36
Horizontal Orientation	36
Vertical Orientation	40
IV CONCLUSIONS	46
Suggested Optimum System	48
BIBLIOGRAPHY	50

Page

APPENDICES 53
APPENDIX A—Fields Program 54
APPENDIX B—Fourier Program 57
APPENDIX C—Time Program 59
APPENDIX D—Mutual Inductance, Coefficient of Coupling Current and Current Derivative Determinations 61
APPENDIX E—V(t) for Different ITS's and I(t) Figures 64
APPENDIX F—Method to Calculate B_z from Experimental Measurements 66
APPENDIX G—Time Output 68
APPENDIX H—Factors Used to Find the Voltage Spectrum of Figure 13 70
APPENDIX I—Proof of Equal Energy and Equal Area of the Square Wave Approximation 73
APPENDIX J—"Student's t" Test 76
APPENDIX K—RMS Error Evaluation 79
APPENDIX L—Definitions of Variables and Operations 82

LIST OF TABLES

Table		Page
1.	Values of $\partial I(t)/\partial t$ for Different ITS's	9
2.	Main Components for Various Repetition Rates	20
3.	Relative Changes in E_x for x,y Positions, Horizontal Orientation	37
4.	Relative E_x Values Corresponding to Figure 32 Coils Vertical z Position as Figure 33	44
5.	Relative E_x Values Corresponding to 0.5 in. Water, Coils Vertical	44
Appendix Tables		
6.	Measured Values of E_x and E_y and Corresponding t Values	78
7.	Values Used in Standard Error Estimates	80
8.	RMS Value of Difference and Measured Average Values	81

LIST OF FIGURES

Figure		Page
1.	Coordinate System	5
2.	Driving Coil System (DCS) and Inductive Test System (ITS) Coils	7
3.	DCS	8
4.	Total EMF of ITS	11
5.	Positive Portion EMF of ITS	11
6.	Theoretical Fields, z = 0 Plane	13
7.	Experimental Fields, z = 0 Plane	14
8.	Theoretical Fields, z = 2cm Plane	15
9.	Experimental Fields, z = 2cm Plane	16
10.	Square Wave Approximation of Burst Used in FOURIER	23
11.	Approximation Single Pulse Waveform	24
12.	Enlargement of the Negative Portion of Figure 11	24
13.	Voltage Spectrum of Figure 11	25
14.	Voltage Spectrum 11Hz Burst	26
15.	Voltage Spectrum 15Hz Burst	27
16.	Voltage Spectrum 20Hz Burst	28
17.	LP Outburst (38kHz)	29
18.	LP Output (one megaHz)	29
19.	DCS Horizontal	31
20.	DCS Vertical	31

Figure		Page
21.	Dipole Fields Measured	32
22.	X,Y Positions Coils Horizontal	33
23.	Cylindrical Positions Coils Horizontal	34
24.	Dipole EMF Position 14, z=0	35
25.	Dipole EMF Position 25, z=3.5cm	35
26.	Dipole EMF Position 25, z=2.3cm	35
27.	z Positions Both Containers Coils Normal	37
28.	Field Plot for Positions of Figure 21	38
29.	E_ϕ Plot Cylindrical Boundaries	39
30.	Comparison of E_y and E_z for Horizontal and Vertical Orientations	41
31.	Plane x,y at z = 2.5 in.	42
32.	Positions Coils Vertical	43
33.	Relative z Position and Water Level	43
34.	$\bar{E}$ Lines for Vertical Coils	46
35.	Vertical Coils	47
36.	Horizontal Coils	48
37.	Proposed Optimum Boundary	49
38.	Proposed Optimum for Cells	49
Appendix Figures		
39.	DCS Schematic	62
40.	Circuit to Find M	62

Figure		Page
41.	Circuit to Find M	62
42.	V(t) LITS of 2.0 microHenerys	65
43.	V(t) LITS of 4.0 microHenerys	65
44.	I(t)	65
45.	Time Output 11Hz Burst	69
46.	Waveform Used to Compute Real and Imaginary Parts	72
47.	Voltage and Current Waveforms Equal Energy Calculations	75

ABSTRACT

The subject of this thesis is to measure spatial variations of electromagnetic fields from circular time varying current sources. In order to verify experimental measurements digital computer models of the fields in free space were derived. Fields within Ringer's solution contained within cylindrical and rectangular boundaries were measured experimentally. It was found that neither boundary provides for uniform field magnitudes throughout the containers regardless of the direction of the applied magnetic field from the circular current loops. A coaxial cylindrical container was suggested as a means of providing more uniform fields throughout the solution.

A brief Fourier analysis of several types of waveforms induced in the Ringer's solution was also performed.

INTRODUCTION

Electromagnetic energy has been shown to be a catalyst to certain functions of selected biological systems. These catalytic properties are now being used clinically to heal recalcitrant bone fractures. Several researchers have conducted numerous experiments testing the effects of electromagnetic energy on biological systems [1,2,3]. Some systems Dr. A. A. Pilla has tested include: calcium uptake in embryonic chick tibia [4], modulation of rat radial osteotomy repair (with P. Christel and G. Cerf)[5], and lifespan extension (electromagnetic energy in addition to chemotherapy for positive results, with Dr. Steve Smith) of rats with melanomas [6]. Because Pilla used induced energy as opposed to dc delivered by metal conductors, the possibility of a chemical reaction between the system and the apparatus used to apply energy is eliminated.

Certain experiments of Pilla's have shown that slight changes in waveforms applied to biological systems produce dramatically different results. For example, by changing only the repetition rate of a five msec, burst type waveform, percent change versus controls vary from slightly negative to largely positive [5]. Although some Fourier analysis was done in order to determine an approximate upper frequency limit of the spectral components of the waveform, it did not become clear why different waveforms caused different results.

When cells are exposed to induced energy the question arises: are all cells throughout the system exposed to the same magnitudes of $\bar{E}$, the electric field intensity vector, as well as $\bar{H}$, the magnetic field intensity vector? Obtaining boundary conditions such that all cells of the system are exposed to uniform magnitude $\bar{E}$ and $\bar{H}$ could contribute to the study of biological response versus magnitudes of the induced fields. Further, Gandhi [7] has indi-

cated that the direction of a propagating wave could be significant in regards to biological effects. Thus, perhaps knowledge of direction of the fields with respect to individual cells could be important.

The main contribution of this thesis is to study field patterns in homogeneous material within various boundary conditions. Rectangular and cylindrical containers were considered as boundaries for Ringer's solution and electric field patterns within the containers were determined experimentally for different directions of the applied time varying magnetic field. Although not considered in this thesis theoretical models of electric field intensity within the rectangular containers have been derived by Dr. Bruce R. McLeod [8]. Because biological cells introduce a boundary not considered in any measurements or derivations in this thesis, the values of the fields and currents within the cell were not determined. However, this thesis will show that cells at various positions of the system will certainly be exposed to different magnitudes of external currents and fields and the degree of variation of the exposure depends upon position as well as orientation of the biological system.

Chapter I

SPATIAL VARIATIONS OF ELECTRIC AND MAGNETIC FIELDS IN FREE SPACE

Theoretical Fields for Circular Current Loops

In order to obtain theoretical models for $\bar{E}$ and $\bar{B}$, the electric field intensity and magnetic field density vectors respectively, it is appropriate to begin with Maxwell's second equation

$$\nabla \cdot \bar{B} = 0 \tag{1}$$

From Equation 1 through the use of a vector identity it can be shown that

$$\bar{B} = \nabla \times \bar{A} \tag{2}$$

The direction of the applied field and low back EMF dictate that only the phi (ϕ) component of $\bar{A}$ exists, where phi is the direction shown in Figure 1. From symmetry $\partial/\partial\phi = 0$ so it follows that

$$\nabla \cdot \bar{A} = 0 \tag{3}$$

for cylindrical coordinates. Thus, Equations 2 and 3 totally define the vector $\bar{A}$. From Maxwell's third equation,

$$\nabla \times \bar{E} = - \partial\bar{B}/\partial t \tag{4}$$

with the use of Equation 1 and the vector identity, the curl of the gradient of any scalar is identically zero, Equation 5 results

$$\bar{E} = - \nabla V - \partial\bar{A}/\partial t \tag{5}$$

Since $- \nabla V$ is the solution to the homogeneous form of Equation 4, the solution for $\bar{E}$ with $\partial I(t)/\partial t$ as well as $\partial\bar{B}/\partial t$ equal to zero, must be $- \nabla V$. However, since $\rho = 0$, i.e., no

free charge density between the coils as well as at the source, it follows that $V = 0$. Therefore,

$$\bar{E} = - \partial \bar{A}/\partial t \tag{6}$$

The two equations used to determine spatial variations of field quantities in free space, with a circular current loop the source, have been derived as follows [9,10]:

$$A\phi = \frac{\mu I}{k} \left(\frac{a}{r}\right)^{1/2} [(1 - \tfrac{1}{2} k^2)K - E] \tag{7}$$

$$B_z = \frac{\mu I}{2 [(a + r)^2 + z^2]^{1/2}} \left[K + \left(\frac{a^2 - r^2 - z^2}{(a - r)^2 + z^2}\right)E\right] \tag{8}$$

Where: I and a is the current and fixed radius respectively of the loop; $k^2 = 4ar/[(a + r)^2 + z^2]$; μ is the permeability constant; K and E are elliptic integrals of the first and second kinds respectively, and z and r are the running variables of the coordinate system as shown in Figure 1.

It is noted that both of the references cited for Equations 7 and 8 derived them for constant currents. However, they still hold for I replaced by I(t), a time varying current. Also, an equation for the radial component of the magnetic field density vector B_r was given by the references cited. Since B_r was found to be nearly an order of magnitude smaller than B_z in the region of constant B_z, B_r was ignored.

In order to obtain theoretical free space values of B_z and E_ϕ versus position, Equations 7 and 8 were programmed into a digital computer. Since the system was assumed linear, the principle of superposition was used to calculate relative field variations for a fixed z plane versus r. Once the magnitudes of the field quantities were obtained for two single turn current loops of specific dimensions, scale factors were applied for our case to obtain Figures 6 and 8. The multiplying factors included: the number of turns per coil of the

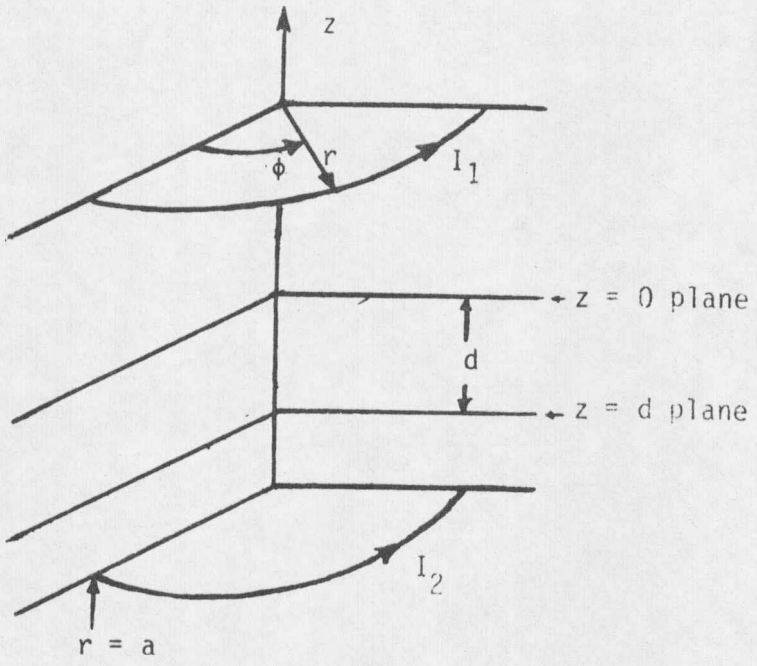

Fig. 1. Coordinate System.

driving coil system (DCS) and the value of the $\partial I(t)/\partial t$ and $I(t)$ at some specific time (t_1) for E_ϕ and B_z respectively. Methods used to determine $I(t)$ and $\partial I(t)/\partial t$ are shown in Appendix D. Also, included in the program (FIELDS) was a subroutine to evaluate elliptic integrals [11]; the program is displayed in Appendix A.

Selection Inductive Test Systems

In order to verify the theoretical equations for E_ϕ and B_z, a method of measurement had to be devised. This section explains the theory used to choose the inductive test systems (ITS's) used to gather data.

The coupling of $\bar{E}$ and $\bar{B}$, as seen in Equation 4, creates the possibility of calculating $\bar{E}$ and $\bar{B}$ as functions of r and z from measurements of the same quantity. From Equation 4 using Stoke's theorem it follows that

$$\oint \bar{E} \cdot \bar{dl} = - \int \frac{\partial \bar{B}}{\partial t} \cdot \bar{ds} = \partial \Phi / \partial t \tag{9}$$

Equation 9 is equal to the induced electromotive force (EMF). However, the different differentials of the two integrals make it convenient to have a separate source of EMF for $\bar{E}$ and $\bar{B}$ determinations. Thus, in order to verify plots obtained theoretically, different sources of EMF were used for $\bar{E}$ and $\bar{B}$.

Although $\bar{E}$ varies with r, z and time it does not vary with ϕ; also, only a ϕ component of $\bar{E}$ exists. Therefore, since

$$\bar{dl} = r \, d\phi \bar{a\phi} \tag{10}$$

and since E_ϕ is a constant of integration in Equation 9 a measured EMF with a proper device allows E_ϕ to be calculated for a particular radius in a constant z plane.

Unfortunately, since B_z varies with respect to r, B_z is not a constant of integration. However, assuming the theoretical plots to be correct (Figures 6 and 8), B_z is nearly constant for the range of r from zero to four centimeters. Therefore, B_z was assumed constant with respect to integration in that range and a suitable differential is

$$\bar{ds} = r' \, dr' \, d\phi' \bar{az} \tag{11}$$

Primed variables indicate that the center of the $\bar{ds}$ did not necessarily coincide with the center of the coordinate system of the DCS as shown in Figure 2.